Available online at www.sciencedirect.com
ScienceDirect
Journal of Sound and Vibration 309 (2008) 52–62
JOURNAL OF SOUND AND VIBRATION
www.elsevier.com/locate/jsvi

Study of the scattering of nonlinearly interacting plane acoustic waves by an elongated spheroid

Iftikhar B. Abbasov*

Taganrog State Radio Engineering University, Nekrasovskyi 44, 347928 Taganrog, Russian Federation

Received 24 June 2003; received in revised form 13 March 2007; accepted 14 March 2007
Available online 24 September 2007

Abstract

The scattering of nonlinearly interacting plane acoustic waves on a rigid elongated spheroid is considered. The foci of the spheroid coincide with foci of the spheroidal coordinate system. The method of successive approximations is used to obtain the solutions to the inhomogeneous wave equation in the first and second approximations. Asymptotic expressions are offered for the components of the total acoustic pressure of the difference frequency wave, and the scattering diagrams for these components are presented.

1. Introduction

The problem of scattering of acoustic waves by elongated spheroids was formulated for the first time in Refs. [1,2]. In these studies, angular characteristics of the acoustic waves scattering by a soft and rigid elongated spheroid were presented. The scattering of plane acoustic waves by thin, acoustically rigid and resilient bodies of revolution was considered in Refs. [3,4]. The problem of plane acoustic wave diffraction by a finite elongated resilient body of revolution was investigated in Ref. [5]. Here, asymptotic expressions for the scattered field were derived. The problem of plane acoustic wave scattering by spheroidal shells was considered in Refs. [6,7]. In contrast to previous works, these investigations research the surface waves reflected by the scatterers. Several experimental studies of acoustic waves scattered by elongated bodies were discussed in Refs. [8,9]. However, the problem of the interacting nonlinear acoustic waves scattered by an elongated spheroid has not been examined. This problem arises when an acoustic parametric array is used for sonar applications. In many practical cases, natural and artificial objects can be presented as the spheroidal scattering objects. One example is sea cetaceans. This problem can also become important when coastal ecological monitoring is carried out. This paper presents a study of scattering the nonlinearly interacting plane acoustic waves by a rigid elongated spheroid.

2. Theory

To present the problem, the system of elongated spheroidal coordinates ξ, η, φ was chosen. The foci of the spheroid coincide with the foci of the spheroidal coordinate system. The spheroid is formed by the

*Tel.: +7 863 43 7 17 94; fax: +7 863 44 6 50 19.
E-mail address: igkd@egf.tsure.ru.

0022-460X/$ - see front matter © 2007 Elsevier Ltd. All rights reserved.
doi:10.1016/j.jsv.2007.03.060

ellipse ξ_0 rotated about a major axis, which coincides with the x-axis of the Cartesian system. The geometry of the problem is presented in Fig. 1. The coordinate surfaces are for the spheroids-$\xi = \text{const}$ and for the two-sheeted hyperboloids-$\eta = \text{const}$.

Elongated spheroidal coordinates are related to Cartesian coordinates by the following expressions [10]:

$$x = h_0\xi\eta, \quad y = h_0\sqrt{(\xi^2-1)(1-\eta^2)}\cos\varphi, \quad z = h_0\sqrt{(\xi^2-1)(1-\eta^2)}\sin\varphi,$$

where $h_0 = d/2$ and d is the interfocal distance. Spheroidal coordinates ξ, η, φ are considered within the limits: $1 \leqslant \xi < \infty$; $-1 \leqslant \eta \leqslant 1$; $0 \leqslant \varphi \leqslant 2\pi$.

The perfect spheroid was put into homogeneous medium. The spheroid's surface is characterized by the coordinate ξ_0. Assuming that interacting plane high-frequency acoustic waves of the unit pressure amplitude falls on the spheroid at an arbitrary polar angle θ_0 ($\theta_0 = \arccos\eta_0$) and an azimuthal angle φ_0, we express the acoustic pressure as

$$p_{ni} = \exp[-\mathrm{i}(k_n r_0 \cos\theta_0 - \omega_n t)], \tag{1}$$

where k_n, is the wavenumber, $n = 1,2$ according to the waves with frequencies ω_1 and ω_2, and r_0 is the radius-vector of the polar coordinate system.

Consider an incident plane wave in the spheroidal coordinate system [11]:

$$\exp[\mathrm{i}(\omega_n t - k_n r_0 \cos\theta_0)] = -2\exp(\mathrm{i}\omega_n t)\sum_{m=0}^{\infty}\sum_{l\geqslant m}^{\infty}\mathrm{i}^{-l}\overline{S_{ml}}(k_n h_0,\eta_0)\overline{S_{ml}}(k_n h_0,\eta)R_{ml}^{(1)}(k_n h_0,\xi)\cos m(\varphi-\varphi_0),$$

where $\overline{S_{ml}}(k_n h_0,\eta)$ Is the normalized angular first-order function and $R_{ml}^{(1)}(k_n h_0,\xi)$ is the radial spheroidal first-order function.

After the plane wave scattering on the spheroid, the scattered spheroidal wave of pressure will propagate as an outgoing wave [12]

$$p_{ns}(\xi,\eta,\varphi) = 2\exp(\mathrm{i}\omega_n t)\sum_{m=0}^{\infty}\sum_{l\geqslant m}^{\infty}A_{ml}(k_n h_0,\xi_0)\overline{S_{ml}}(k_n h_0,\eta)R_{ml}^{(3)}(k_n h_0,\xi)\cos m\varphi, \tag{2}$$

where the coefficient $A_{ml}(k_n h_0,\xi_0)$ is dependent on boundary conditions on the spheroid surface and $R_{ml}^{(3)}(k_n h_0,\xi)$ is the radial spheroidal third-order function.

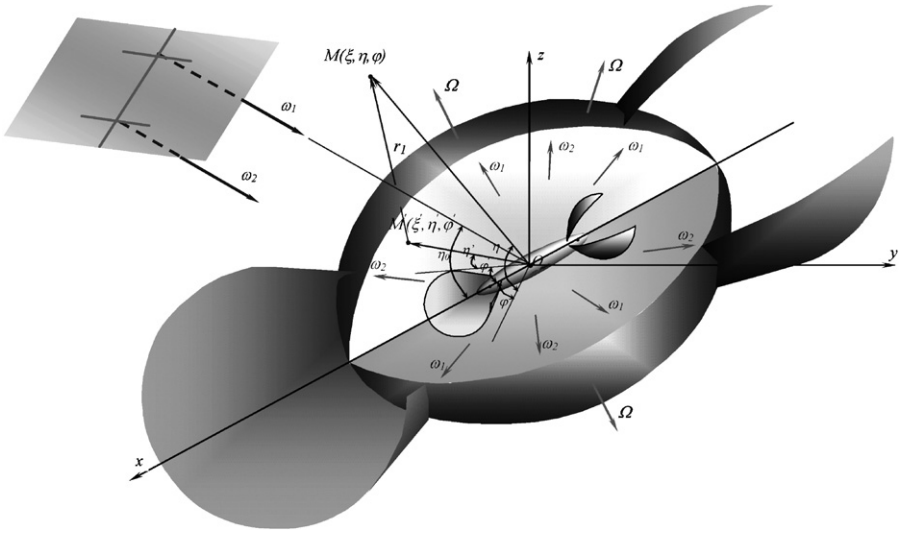

Fig. 1. Geometry of the problem.

In this case, the spheroid is considered to be acoustically rigid, so the Neumann boundary condition must be applied on the surface

$$\left(\frac{\partial p_{ni}}{\partial n}+\frac{\partial p_{ns}}{\partial n}\right)\Bigg|_{\xi=\xi_0}=0 \tag{3}$$

and the coefficient $A_{ml}(k_nh_0,\xi_0)$ will be determined by the following expression:

$$A_{ml}(k_nh_0,\xi_0)=-\mathrm{i}^l\varepsilon_m\overline{S_{ml}}(k_nh_0,\eta_0)\frac{R_{ml}^{(1)'}(k_nh_0,\xi_0)}{R_{ml}^{(3)'}(k_nh_0,\xi_0)},$$

where $R_{ml}^{(1)'}(k_nh_0,\xi_0)$ and $R_{ml}^{(3)'}(k_nh_0,\xi_0)$ are the derivatives of the first- and third-order functions, $\varepsilon_m=1$ for $m=0$, $\varepsilon_m=2$ for $m>0$.

With the appearance of the scattered spheroidal wave, the total acoustic pressure of the primary field around the spheroid will have the form

$$\begin{aligned}p^{(1)}=p_{ni}+p_{ns}=&\left[\sum_{m=0}^{\infty}\sum_{l\geqslant m}^{\infty}B_{ml}(k_nh_0)\exp\left[\mathrm{i}(\omega_nt-l\pi/2)\right]+\sum_{m=0}^{\infty}\sum_{l\geqslant m}^{\infty}D_{ml}(k_nh_0)\exp[\mathrm{i}(\omega_nt-m\varphi)]\right]\\&+\left[\sum_{m=0}^{\infty}\sum_{l\geqslant m}^{\infty}B_{ml}(k_nh_0)\exp\left[-\mathrm{i}(\omega_nt-l\pi/2)\right]+\sum_{m=0}^{\infty}\sum_{l\geqslant m}^{\infty}D_{ml}(k_nh_0)\exp[-\mathrm{i}(\omega_nt-m\varphi)]\right],\end{aligned} \tag{4}$$

where

$$\begin{aligned}B_{ml}(k_nh_0)&=2\overline{S_{ml}}(k_nh_0,\eta_0)\overline{S_{ml}}(k_nh_0,\eta)R_{ml}^{(1)}(k_nh_0,\xi)\cos m(\varphi-\varphi_0),\\D_{ml}(k_nh_0)&=2A_{ml}(k_nh_0,\xi_0)\overline{S_{ml}}(k_nh_0,\eta_0)R_{ml}^{(3)}(k_nh_0,\xi)\cos m\varphi.\end{aligned}$$

To solve the problem of the nonlinear interaction of the primary high-frequency waves, we combine expression (4) with its complex-conjugate part.

Nonlinear wave processes between incident and scattered waves surrounding the spheroid can be described with the inhomogeneous wave equation [13]

$$\nabla^2p^{(2)}-\frac{1}{c_0^2}\frac{\partial^2p^{(2)}}{\partial t^2}=-Q=-\frac{\varepsilon}{c_0^4\rho_0}\frac{\partial^2{p^{(1)}}^2}{\partial t^2}, \tag{5}$$

where Q is the volume density of the sources of secondary waves, c_0 the sound velocity in the medium, ε the quadratic nonlinearity parameter, ρ_0 the density of the unperturbed medium, and $\rho^{(1)}$ and $\rho^{(2)}$ the total acoustic pressures of the primary and secondary fields.

It is important to note that the waves of the primary field are the high-frequency waves: incident plane waves p_i and scattered spheroidal waves p_s with angular frequencies ω_1 and ω_2. The waves of the secondary field are the waves that appear as a result of the nonlinear interaction of initial high-frequency waves. This includes the difference frequency wave $\omega_2-\omega_1=\Omega$, the summation frequency wave $\omega_2+\omega_1$, and the second harmonic waves $2\omega_1$, $2\omega_2$.

The wave equation (5) is solved by the method of successive approximations. In the first approximation, the solution is represented by expression (4) for the total acoustic pressure of the primary field $p^{(1)}$. To determine solution in the second approximation $p^{(2)}$, the right-hand side of Eq. (5) should feature four frequency components: second harmonics of the incident waves ($2\omega_1$, $2\omega_2$) and ($\omega_1+\omega_2$, $\omega_2-\omega_1=\Omega$).

The expression for the volume density of secondary waves sources at the difference frequency Ω is

$$\begin{aligned}Q_-=\frac{2\Omega^2\varepsilon}{c_0^4\rho_0}&\left[\sum_{m=0}^{\infty}\sum_{l\geqslant m}^{\infty}B_{ml}(k_1h_0)B_{ml}(k_2h_0)\cos\,\Omega t+\sum_{m=0}^{\infty}\sum_{l\geqslant m}^{\infty}B_{ml}(k_1h_0)D_{ml}(k_2h_0)\,\cos\left(\Omega t+l\pi/2-m\varphi\right)\right.\\&\left.+\sum_{m=0}^{\infty}\sum_{l\geqslant m}^{\infty}B_{ml}(k_2h_0)D_{ml}(k_1h_0)\cos(\Omega t+m\varphi-l\pi/2)+\sum_{m=0}^{\infty}\sum_{l\geqslant m}^{\infty}D_{ml}(k_1h_0)D_{ml}(k_2h_0)\cos\,\Omega t\right].\end{aligned} \tag{6}$$

To solve the inhomogeneous wave equation (5) with the right-hand side given by Eq. (6) in the second approximation, we seek the solution in the complex form

$$p_-^{(2)} = \frac{1}{2} P_-^{(2)} \exp(\mathrm{i}(\Omega t + \delta) + (\mathrm{c.}\tilde{n}.)). \tag{7}$$

Substitution of expression (7) into the inhomogeneous wave equation (5) gives the inhomogeneous Helmholtz equation

$$\nabla^2 P_-^{(2)} + k_-^2 P_-^{(2)} = -q_-(\xi, \eta, \varphi), \tag{8}$$

where k_- is the wavenumber of the difference frequency Ω, and

$$\begin{aligned} q_-(\xi,\eta,\varphi) = \frac{2\Omega^2\varepsilon}{c_0^4\rho_0}\Bigg[&\sum_{m=0}^{\infty}\sum_{l\geqslant m}^{\infty} B_{ml}(k_1h_0)B_{ml}(k_2h_0)\exp(\mathrm{i}\Omega t) \\ &+ \sum_{m=0}^{\infty}\sum_{l\geqslant m}^{\infty} B_{ml}(k_1h_0)D_{ml}(k_2h_0)\exp\left[\mathrm{i}(\Omega t + l\pi/2 - m\varphi)\right] \\ &+ \sum_{m=0}^{\infty}\sum_{l\geqslant m}^{\infty} B_{ml}(k_2h_0)D_{ml}(k_1h_0)\exp\left[\mathrm{i}(\Omega t + m\varphi - l\pi/2)\right] \\ &+ \sum_{m=0}^{\infty}\sum_{l\geqslant m}^{\infty} D_{ml}(k_1h_0)D_{ml}(k_2h_0)\exp(\mathrm{i}\Omega t)\Bigg]. \end{aligned}$$

The solution to the inhomogeneous Helmholts equation (8) has the form of a volume integral of the product of the Green function with the density of the secondary wave sources [13,14]:

$$P_-^{(2)}(\xi,\eta,\varphi) = \int_V q_-(\xi',\eta',\varphi')G(r_1)h_{\xi'}h_{\eta'}h_{\varphi'}\,\mathrm{d}\xi'\,\mathrm{d}\eta'\,\mathrm{d}\varphi', \tag{9}$$

where $G(r_1)$ is the Green function, r_1 the distance between the current point of the volume $M'(\xi',\eta',\varphi')$ and the observation point $M(\xi,\eta,\varphi)$ (Fig. 1), and $h_{\xi'}, h_{\eta'}, h_{\varphi'}$ are the scale factors [15]:

$$h_{\xi'} = h_0\sqrt{\frac{\xi'^2-\eta'^2}{\xi'^2-1}}, \quad h_{\eta'} = h_0\sqrt{\frac{\xi'^2-\eta'^2}{1-\eta'^2}}, \quad h_{\varphi'} = h_0\sqrt{(\xi'^2-1)(1-\eta'^2)}.$$

In the far field $r' \ll r$, the Green function is determined by the asymptotic expression

$$G(r_1) = \exp(-\mathrm{i}k_-r_1)/r_1 \approx \exp\left[-\mathrm{i}k_-\left(h_0\xi - h_0\xi'\eta\eta' - h_0\xi'\sqrt{(1-\eta^2)(1-\eta'^2)}\right)\right]\Big/ h_0\xi.$$

The integration in Eq. (9) is performed over the volume V occupied by the second wave sources and bounded in the spheroidal coordinates by the relations

$$\xi_0 \leqslant \xi' \leqslant \xi_S, \quad -1 \leqslant \eta' \leqslant 1, \quad 0 \leqslant \varphi' \leqslant 2\pi.$$

This volume has the form of a spheroidal layer of the medium, stretching from the spheroid's surface to the nonlinear interaction boundary (Fig. 1). An external spheroid with coordinate ξ_S appears to be the boundary of this area. Coordinate ξ_S is defined by the size of the nonlinear interaction area between the initial high-frequency waves. This size is inversely proportional to the coefficient of viscous sound attention associated with the corresponding pumping frequency. Beyond this area, the initial waves are assumed to attenuate linearly.

After the integration with respect to coordinates φ' and η' (considering the high-frequency approximation), Eq. (9) takes the form

$$\begin{aligned} P_-^{(2)}(\xi,\eta,\varphi) &= P_{-1}^{(2)}(\xi,\eta,\varphi) + P_{-2}^{(2)}(\xi,\eta,\varphi) + P_{-3}^{(2)}(\xi,\eta,\varphi) + P_{-4}^{(2)}(\xi,\eta,\varphi) \\ &= C_-\frac{1}{k_-h_0\eta}\left[\int_{\xi_0}^{\xi_S} T\xi' \sin(k_-h_0\xi'\eta)\,\mathrm{d}\xi' - \int_{\xi_0}^{\xi_S} T\frac{\sin(k_-h_0\xi'\eta)}{\xi'}\,\mathrm{d}\xi'\right], \end{aligned} \tag{10}$$

where

$$C_- = \frac{8h_0^2\pi\Omega^2\varepsilon\exp(-\mathrm{i}k_-h_0\xi)}{c_0^4\rho_0\xi},$$

$$T = \left[\sum_{m=0}^{\infty}\sum_{l\geqslant m}^{\infty} B_{ml}(k_1h_0)B_{ml}(k_2h_0) + \sum_{m=0}^{\infty}\sum_{l\geqslant m}^{\infty} B_{ml}(k_1h_0)D_{ml}(k_2h_0)\exp\left[\mathrm{i}(l\pi/2 - m\varphi)\right]\right.$$
$$\left. + \sum_{m=0}^{\infty}\sum_{l\geqslant m}^{\infty} B_{ml}(k_2h_0)D_{ml}(k_1h_0)\exp\left[\mathrm{i}(m\varphi - l\pi/2)\right] + \sum_{m=0}^{\infty}\sum_{l\geqslant m}^{\infty} D_{ml}(k_1h_0)D_{ml}(k_2h_0)\right]$$

(from here on, the time factor $\exp(\mathrm{i}\Omega t)$ is omitted).

Expression (10) for the total acoustic pressure of the difference-frequency wave $P_-^{(2)}(\xi,\eta,\varphi)$ consists of four spatial components. The first component $P_{-1}^{(2)}(\xi,\eta,\varphi)$ corresponds to the part of the acoustic pressure of the difference-frequency wave, that is formed in the spheroidal layer of the nonlinear interaction area by the incident high-frequency plane waves ω_1 and ω_2. The second component $P_{-2}^{(2)}(\xi,\eta,\varphi)$ describes the interaction of the incident plane wave of frequency ω_1 with the scattered spheroidal wave of frequency ω_2. The third component $P_{-3}^{(2)}(\xi,\eta,\varphi)$ corresponds to the interaction of the scattered plane wave of frequency ω_2 with the scattered spheroidal wave of ω_1. The fourth component $P_{-4}^{(2)}(\xi,\eta,\varphi)$ characterises the interaction of two scattered spheroidal waves with frequencies ω_1 and ω_2.

3. Results

To obtain the final expression of the total acoustic pressure of the difference-frequency wave $P_-^{(2)}(\xi,\eta,\varphi)$, consider the first spatial component $P_{-1}^{(2)}(\xi,\eta,\varphi)$ from Eq. (10), which characterizes the nonlinear interaction between incident plane waves of high frequency

$$P_{-1}^{(2)}(\xi,\eta,\varphi) = \frac{C_-}{k_-h_0\eta}\left[\int_{\xi_0}^{\xi_S}\sum_{m=0}^{\infty}\sum_{l\geqslant m}^{\infty} B_{ml}(k_1h_0)B_{ml}(k_2h_0)\xi'\,\sin(k_-h_0\xi'\eta)\,\mathrm{d}\xi'\right.$$
$$\left. - \int_{\xi_0}^{\xi_S}\sum_{m=0}^{\infty}\sum_{l\geqslant m}^{\infty} B_{ml}(k_1h_0)B_{ml}(k_2h_0)\frac{\sin(k_-h_0\xi'\eta)}{\xi'}\,\mathrm{d}\xi'\right]. \tag{11}$$

It should be noted that this is the only component that gives no information about the scatterer. The boundaries of the integration layer are directly defined by the elongated spheroid shape.

Using representation of the plane wave in the spheroidal coordinate system and substituting $B_{ml}(k_nh_0)$, expression (11) takes the form

$$P_{-1}^{(2)}(\xi,\eta,\varphi) = \frac{C_-}{k_-h_0\eta}\left[\int_{\xi_0}^{\xi_S}\exp\left[-\mathrm{i}k_-h_0\xi'\eta\right]\xi'\,\sin(k_-h_0\xi'\eta)\,\mathrm{d}\xi' - \int_{\xi_0}^{\xi_S}\exp\left[-\mathrm{i}k_-h_0\xi'\eta\right]\frac{\sin(k_-h_0\xi'\eta)}{\xi'}\,\mathrm{d}\xi'\right]. \tag{12}$$

After the final integration wit respect to the coordinate ξ', the expression for the first component (12) has the form

$$P_{-1}^{(2)}(\xi,\eta,\varphi) = P_{-11}^{(2)} + P_{-12}^{(2)} + P_{-13}^{(2)} + P_{-14}^{(2)}, \tag{13}$$

where

$$P_{-11,-12}^{(2)} \approx \mp\frac{C_-}{2k_-^2h_0^2\eta(\eta_0\mp\eta)}\left[\xi_S\exp\left[\mathrm{i}k_-h_0(\eta_0\mp\eta)\xi_S\right] - \xi_0\exp\left[\mathrm{i}k_-h_0(\eta_0\mp\eta)\xi_0\right]\right],$$
$$P_{-13,-14}^{(2)} \approx \mp\frac{C_-}{2\mathrm{i}}\left[-E\mathrm{i}\left[-\mathrm{i}k_-h_0(\eta_0\mp\eta)\xi_S\right] + E\mathrm{i}\left[-\mathrm{i}k_-h_0(\eta_0\mp\eta)\xi_0\right]\right]$$

and $E\mathrm{i}(ax) = \int((\exp(ax))/x)\,\mathrm{d}x$ is the integral exponential function.

From expression (13) for the first component $P_{-1}^{(2)}(\xi,\eta,\varphi)$ of the total acoustic pressure of the difference-frequency wave, it follows that the scattering diagram of this component is determined by the function

$1/(\eta_0 \pm \eta)$. This function depends on the coordinate η_0 or, the polar coordinate system, equivalent to the angle of incidence θ_0 of the highfrequency plane waves. The scattering diagrams of the first component $P^{(2)}_{-1}(\xi,\eta,\varphi)$ are shown in Fig. 2 for angles of incidence of the high-frequency plane waves $\theta_0 = 30^\circ$ ($k_- h_0 = 5$), and $\theta_0 = 0^\circ$ ($k_- h_0 = 0.5$).

In the direction of the angle of incidence (with respect to the z-axis), the scattering diagrams have major maximums. Increase of the amplitude of the spheroidal wave produced by the scatterer leads to additional maximums in lateral directions (irrespective of the angle of incidence). This result is connected with the increase of the function $1/\eta$. Increasing the extent of the interaction region (the coordinate ξ_S) results in the narrowing of the scattering lobes; this scenario corresponds to increasing the size of the re-radiating volume around the scatterer.

The elongated spheroid has radial dimension $\xi_0 = 1.005$ with the semi-axes correlation 1:10. Acoustic pressure of the difference frequency wave has been calculated in the far field of the scattering spheroid, i.e. in the Fraunhofer region. Therefore, the scattering field can be considered as being shaped by. Shadowing of the secondary waves sources by the scatterer itself can occur in the Rayleigh region. Here, it is necessary to take into account wave dimensions of the scatterer as well as the distance to the point of observation $M(\xi,\eta,\varphi)$. In the cases presented in this contribution, the point of observation was at radial distances $\xi = 7$ and 15, which exceeded the length of the elongated spheroid by an order magnitude.

Now consider the second $P^{(2)}_{-2}(\xi,\eta,\varphi)$ and third $P^{(2)}_{-3}(\xi,\eta,\varphi)$ components from Eq. (10) for the total acoustic pressure of the difference-frequency wave, these components characterise the nonlinear interaction of the incident plane waves with the scattered spheroidal ones waves:

$$P^{(2)}_{-2}(\xi,\eta,\varphi) = \frac{C_-}{k_- h_0 \eta}\left[\int_{\xi_0}^{\xi_S} \sum_{m=0}^{\infty}\sum_{l\geqslant m}^{\infty} B_{ml}(k_1 h_0) D_{ml}(k_2 h_0) \exp\left[\mathrm{i}(l\pi/2 - m\varphi)\right] \xi' \, \sin(k_- h_0 \xi' \eta)\, \mathrm{d}\xi' \right.$$
$$\left. - \int_{\xi_0}^{\xi_S} \sum_{m=0}^{\infty}\sum_{l\geqslant m}^{\infty} B_{ml}(k_1 h_0) D_{ml}(k_2 h_0) \exp\left[\mathrm{i}(l\pi/2 - m\varphi)\right] \frac{\sin(k_- h_0 \xi' \eta)}{\xi'}\, \mathrm{d}\xi' \right]. \tag{14}$$

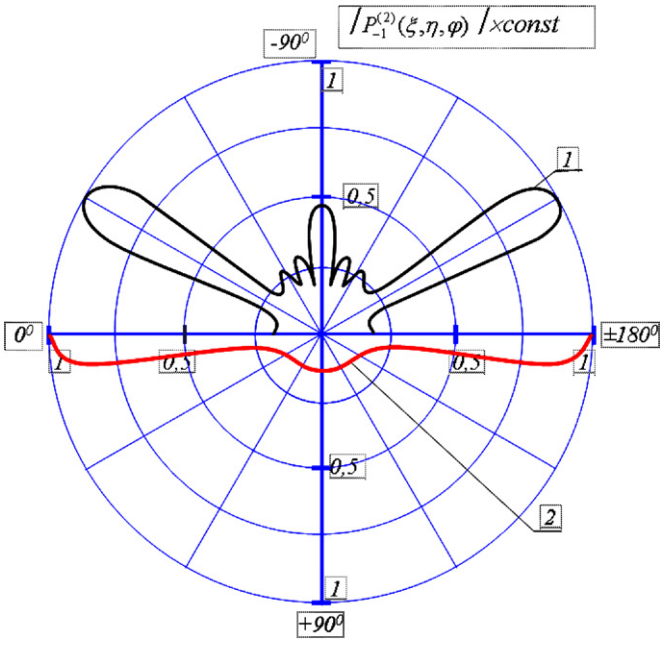

Fig. 2. Scattering diagrams of the spatial component $P^{(2)}_{-1}(\xi,\eta,\varphi)$ of the total acoustic pressure produced by the difference-frequency wave by a rigid elongated spheroid for $f_2 = 1000$ kHz, $k_{1,2}h_0 \approx 40$, $h_0 = 0.01$ M, $\xi_0 = 1.005$ (relations axis-1:10), $\xi = 7$, (1) $f_1 = 880$ kHz, $F_- = 120$ kHz, $k_- h_0 = 5$, $\theta_0 = 30^\circ$, (2) $f_1 = 988$ kHz, $F_- = 12$ kHz, $k_- h_0 = 0.5$, $\theta_0 = 0^\circ$.

Values of $B_{ml}(k_nh_0)$ and $D_{ml}(k_nh_0)$ are substituted into Eq. (14) and the plane wave expansion is used. For the axially symmetrical scattering problem (perfect spheroid), the high-frequency asymptotic forms the angular spheroidal 1st-order function $S_{ml}(k_nh_0,\eta)$ and the radial spheroidal 3rd-order function $R^{(3)}_{ml}(k_nh_0,\xi')$ [12,16]

$$R^{(3)}_{ml}(k_nh_0,\xi') \underset{k_nh_0\xi'\to\infty}{\approx} \frac{i^{-l-1}}{k_nh_0\xi'}\exp\left[ik_nh_0\xi'\right].$$

Then Eq. (11) takes the form

$$P^{(2)}_{-2}(\xi,\eta,\varphi) \approx \frac{2iC_-A(k_2h_0)}{k_-k_2h_0^2\eta\sqrt{2(1-\eta)}}\left[\int_{\xi_0}^{\xi_S}\exp\left[-i(k_2h_0-k_1h_0\eta_0)\xi'\right]\sin(k_-h_0\xi'\eta)\,d\xi' - \int_{\xi_0}^{\xi_S}\exp\left[-i(k_2h_0-k_1h_0\eta_0)\xi'\right]\frac{\sin(k_-h_0\xi'\eta)}{\xi'^2}\,d\xi'\right]. \tag{15}$$

After the final integration [17], the expression for the 2nd component of the total acoustic pressure of the difference-frequency wave takes the form

$$P^{(2)}_{-2}(\xi,\eta,\varphi) = P^{(2)}_{-21} + P^{(2)}_{-22} + P^{(2)}_{-23} + P^{(2)}_{-24}, \tag{16}$$

where

$$P^{(2)}_{-21,-22} \approx \mp\frac{iC_-A(k_2h_0)}{2k_-k_2h_0^2\eta\sqrt{(1-\eta_0)(1-\eta)}}\left[\frac{\exp(iu_2\xi_S)-\exp(iu_2\xi_0)}{u_2}\right],$$

$$P^{(2)}_{-23,-24} \approx \mp\frac{C_-A(k_2h_0)}{2k_-k_2h_0^2\eta\sqrt{(1-\eta_0)(1-\eta)}}\left[\frac{\exp(-iu_2\xi_S)}{\xi_S}-\frac{\exp(iu_2\xi_0)}{\xi_0}-u_2[Ei(-iu_2\xi_S)-Ei(-iu_2\xi_0)]\right],$$

$$u_2 = (k_2h_0 - k_1h_0\eta_0 \mp k_-h_0\eta).$$

The expression for the 3rd component $P^{(2)}_{-3}(\xi,\eta,\varphi)$ is similar to expression (15). An analysis of equation (15) shows that the behaviour of scattering diagrams for the components $P^{(2)}_{-2}(\xi,\eta,\varphi)$ and $P^{(2)}_{-3}(\xi,\eta,\varphi)$ is determined mainly by the function $1/\eta\sqrt{(1-\eta_0)(1-\eta)}$, where the dependence on the angle of incident θ_0 (that is η_0) is not clear. The scattering diagrams of these components are shown in Fig. 3, for $\theta_0 = 30^\circ$ ($k_-h_0 = 5$) and $\theta_0 = 0^\circ$ ($k_-h_0 = 0.5$). These diagrams have maximums in the backward and side directions (0° and $\pm 90^\circ$). The increase of the wave size of the spheroidal scatterer leads to additional maximums, which depend on the angle of incident of the high-frequency plane waves.

Now, we consider the fourth component $P^{(2)}_{-4}(\xi,\eta,\varphi)$ of the total acoustic pressure of the difference-frequency wave. This component characterises the nonlinear interaction of the scattered spheroidal waves with frequencies ω_1 and ω_2:

$$P^{(2)}_{-4}(\xi,\eta,\varphi) = \frac{C_-}{k_-h_0\eta}\left[\int_{\xi_0}^{\xi_S}\sum_{m=0}^{\infty}\sum_{l\geqslant m}^{\infty}D_{ml}(k_1h_0)D_{ml}(k_2h_0)\xi'\,\sin(k_-h_0\xi'\eta)\,d\xi' - \int_{\xi_0}^{\xi_S}\sum_{m=0}^{\infty}\sum_{l\geqslant m}^{\infty}D_{ml}(k_1h_0)D_{ml}(k_2h_0)\frac{\sin(k_-h_0\xi'\eta)}{\xi'}\,d\xi'\right]. \tag{17}$$

After some algebraic manipulations, Eq. (17) takes the form

$$P^{(2)}_{-4}(\xi,\eta,\varphi) = P^{(2)}_{-41} + P^{(2)}_{-42} + P^{(2)}_{-43} + P^{(2)}_{-44}, \tag{18}$$

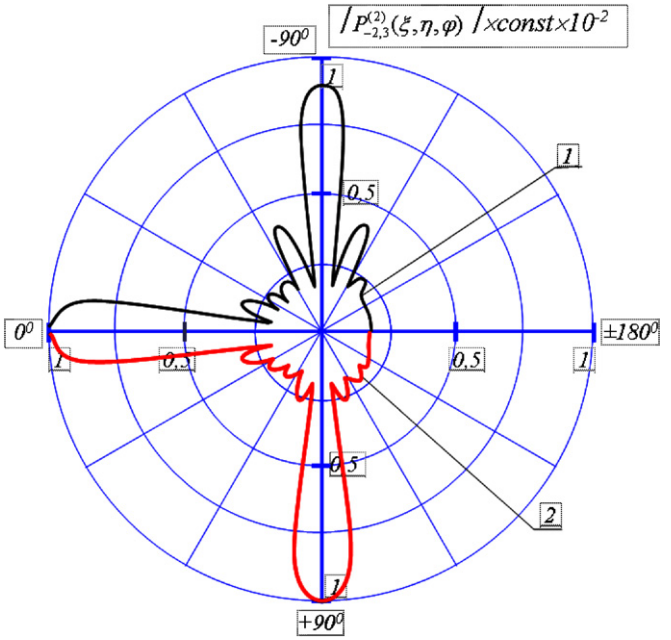

Fig. 3. Scattering diagrams of the spatial components $P^{(2)}_{-2}(\xi,\eta,\varphi)$, $P^{(2)}_{-3}(\xi,\eta,\varphi)$ of the total acoustic pressure produced by the difference-frequency wave by a rigid elongated spheroid for $f_2 = 1000\,\text{kHz}$, $k_{1,2}h_0 \approx 40$, $h_0 = 0.01\,\text{M}$, $\xi_0 = 1.005$, $\xi = 7$, (1) $f_1 = 880\,\text{kHz}$, $F_- = 120\,\text{kHz}$, $k_-h_0 = 5$, $\theta_0 = 30^\circ$, (2) $f_1 = 988\,\text{kHz}$, $F_- = 12\,\text{kHz}$, $k_-h_0 = 0.5$, $\theta_0 = 0^\circ$.

where

$$P^{(2)}_{-41,-42} \approx \mp \frac{C_-A(k_2h_0)A(k_2h_0)}{2ik_-k_2k_1h_0^2\eta(1-\eta_0)(1-\eta)}[-u_4[Ei(-iu_4\xi_S) - Ei(-iu_4\xi_0)]],$$

$$P^{(2)}_{-43,-44} \approx \mp \frac{C_-A(k_2h_0)A(k_2h_0)}{4ik_-k_2k_1h_0^2\eta(1-\eta_0)(1-\eta)}\left[iu_4\left(\frac{\exp(-iu_4\xi_S)}{\xi_S} - \frac{\exp(iu_4\xi_0)}{\xi_0}\right) + u_4^2[Ei(-iu_4\xi_S) - Ei(-iu_4\xi_0)]\right],$$

$$u_4 = (k_-h_0 \mp k_-h_0\eta).$$

The scattering diagrams of the fourth component $P^{(2)}_{-4}(\xi,\eta,\varphi)$ are shown in Fig. 4, for $\theta_0 = 30^\circ$ ($k_-h_0 = 5$) and $\theta_0 = 0^\circ$ ($k_-h_0 = 0.5$). Their configuration is primarily determined by the function $1/\eta(1-\eta_0)(1-\eta)$ of Eq. (18). As indicated above, this function has a maximum in the backward direction and slightly depends on the angle of incidence. Increasing of the spheroidal scatterer wave size results increases lateral scattering.

Fig. 5 presents the scattering diagrams of the total acoustic pressure in the difference-frequency wave $P^{(2)}_-(\xi,\eta,\varphi)$ according to the asymptotic expressions for spatial components. In this case, the angle of incidence is $\theta_0 = 30^\circ$ ($k_-h_0 = 5$) and $\theta_0 = 0^\circ$ ($k_-h_0 = 0.5$), and the coordinate $\xi = 7$.

It is emphasized that the figures illustrate the dependence of acoustic pressure $P^{(2)}_-(\xi,\eta,\varphi)$ on the polar angle $\theta = \arccos\eta$ but not on the angle of asymptote of the hyperbola η. This presentation is conventionally employed for the scattering diagrams in spheroidal coordinates [1–9].

The diagrams are presented in the *xoz* plane (Fig. 1). Polar angle θ varies in the range 0–360°; the value of the angle $\theta = 0^\circ$ corresponds to the position of *x*-axis, and the value $\theta = 90^\circ$ corresponds to *z*-axis. The arrow here shows the direction of the initial plane wave incidence. The axisymmetry of the diagrams with respect to *x*-axis has been taken into account and two diagrams with positive and negative directions of the angle $\theta = \pm 180^\circ$ have been combined.

Fig. 6 shows a spatial simulation of the scattering diagram of the total acoustic pressure $P^{(2)}_-(\xi,\eta,\varphi)$ for $\theta_0 = 30^\circ$ ($k_-h_0 = 5$, $\xi = 7$, an arrow indicates the direction of the initial wave incidence). It is a surface of revolution, and the rotation axis is the larger axis of the elongated spheroid, that is the *x*-axis.

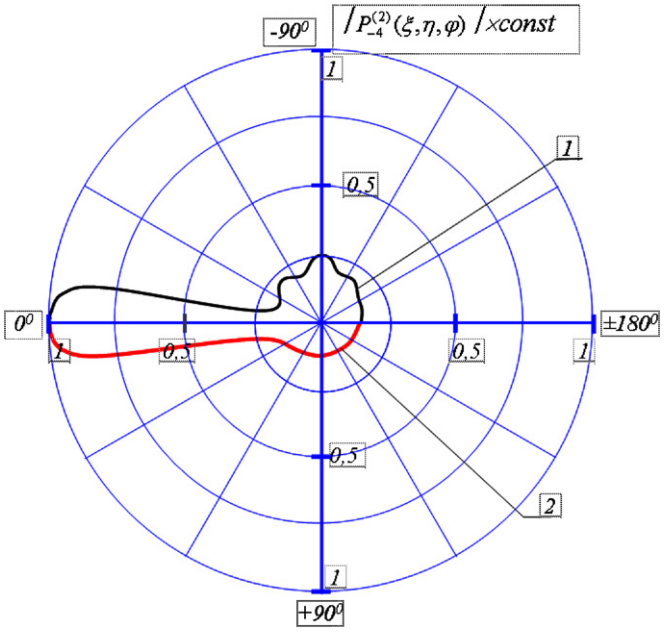

Fig. 4. Scattering diagrams of the spatial component $P_{-4}^{(2)}(\xi,\eta,\varphi)$ of the total acoustic pressure produced by the difference-frequency wave by a rigid elongated spheroid for $f_2 = 1000\,\text{kHz}$, $k_{1,2}h_0 \approx 40$, $h_0 = 0.01\,\text{M}$, $\xi_0 = 1.005$, $\xi = 7$, (1) $f_1 = 880\,\text{kHz}$, $F_- = 120\,\text{kHz}$, $k_-h_0 = 5$, $\theta_0 = 30^\circ$, (2) $f_1 = 988\,\text{kHz}$, $F_- = 12\,\text{kHz}$, $k_-h_0 = 0.5$, $\theta_0 = 0^\circ$.

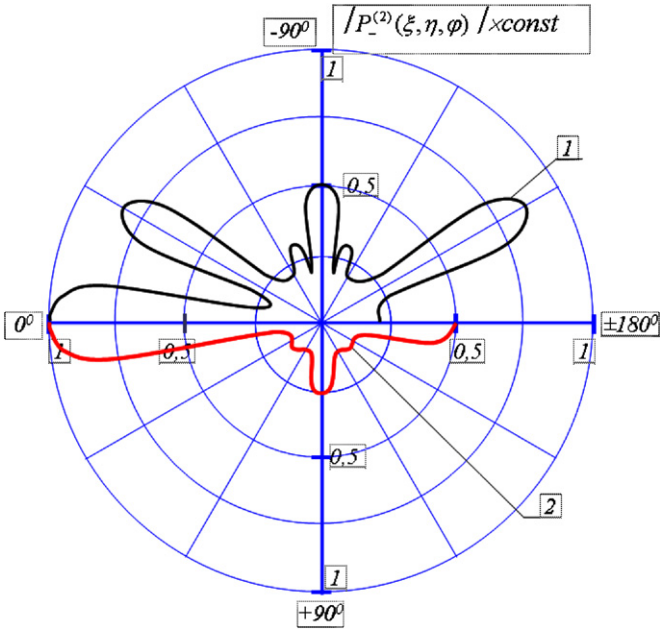

Fig. 5. Scattering diagrams of the total acoustic pressure the difference-frequency wave $P_{-}^{(2)}(\xi,\eta,\varphi)$ by a rigid elongated spheroid for $f_2 = 1000\,\text{kHz}$, $k_{1,2}h_0 \approx 40$, $h_0 = 0.01\,\text{M}$, $\xi_0 = 1.005$, $\xi = 7$, (1) $f_1 = 880\,\text{kHz}$, $F_- = 120\,\text{kHz}$, $k_-h_0 = 5$, $\theta_0 = 30^\circ$, (2) $f_1 = 988\,\text{kHz}$, $F_- = 12\,\text{kHz}$, $k_-h_0 = 0.5$, $\theta_0 = 0^\circ$.

4. Discussion

Although investigation of the linear scattering of acoustic waves by the elongated spheroid has been considered previously, results of the scattering of the nonlinearly interacting acoustic wave were not reported.

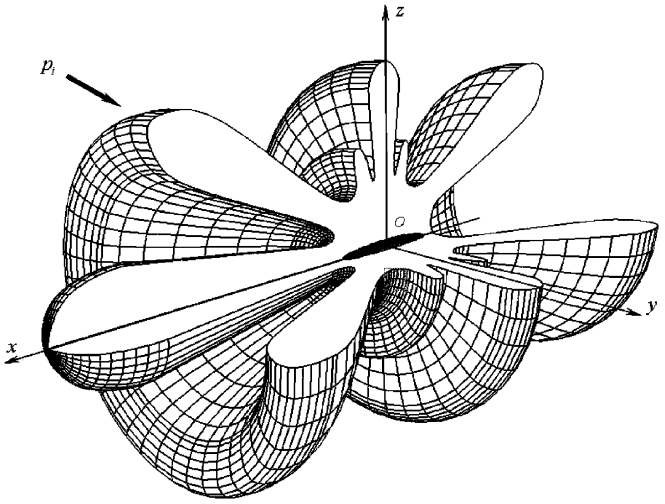

Fig. 6. Spatial model of scattering diagram of the total acoustic pressure the difference-frequency wave $P_{-}^{(2)}(\xi,\eta,\varphi)$ by a rigid elongated spheroid for $f_1 = 880\,\text{kHz}$, $F_{-} = 120\,\text{kHz}$, $k\_h_0 = 5$, $\theta_0 = 30^\circ$, $\xi = 7$.

In most previous publications, the problem is investigated when the angles of incidence of acoustic waves are $\theta = 0^\circ$ and 90° [2–5]. In Eq. [2], the calculated diagrams of plane acoustic wave scattering by a similar size spheroid ($\xi_0 = 1.005$, $kh_0 = 10$) at angle of incidence $\theta = 30^\circ$ are presented. Also in this work the scattering diagram has maximums symmetrical to the angle of incidence (mirror lobes) with respect to z-axis. At angle of incidence $\theta = 0^\circ$ forward scattering dominates [2,4]. The basic maximum is aligned with 140°. When the angle of incidence is $\theta = 90^\circ$ (lateral incidence), there are only two maximums—forward and backward.

An analysis of the acoustic pressure distribution of the difference-frequency wave scattered field shows that the scattering diagrams have maximums in a backward direction. In direction to the angle of incidence, in lateral and transverse directions, plane waves have maximums. Incident high-frequency plane waves form the scattering field in backward and forward directions, and scattered spheroidal waves form the scattering field in transverse direction. An increase in the wave size of the spheroidal scatterer changes maximum levels, and an increase in the size of the interacting area around the elongated spheroidal scatterer leads to narrowing of these maximums.

It is important to note that in this work we considered the case when the scattered field is generated by the secondary wave sources located in the volume around the spheroid. In the case of the linear scattering, these sources are located on the surface of the spheroid. The mirror maximums 30° and 150° appear as a result of the asymptotics of the first spatial sum $P_{-1}^{(2)}(\xi,\eta,\varphi)$ as confirmed in Ref. [2]. Therefore, the plotted scattering diagrams are in conformity with the results of [2–5].

As for the numerical evaluation of the acoustic pressure, it is necessary to note the following. In view of the complexity of mathematical calculations, the obtained asymptotics allow for qualitative evaluation of the spatial distribution of the acoustic pressure in the scattered field. It would be more adequate to compare the results with experimental data. Unfortunately, experiments in nonlinear conditions have not been carried out. For the sake of better understanding of contribution of the separated sums into the cumulative acoustic field, results were presented for two values of the wave dimension and the angle of incidence.

It should be noted, that description of wave processes in spheroidal coordinates have several peculiarities. For example, comparing the acoustic pressure distribution at the distance from the scatterer, the results given in Refs. [18,19] can be taken. Spheroidal coordinates in a far-field transform into spherical ones ($h_0 \to 0$) and $P_{-}^{(2)}(\xi,\eta,\varphi) \to P_{-}^{(2)}(r,\theta,\varphi)$. The results of this research are in agreement with results of prior studies of the scattering process described in spherical coordinates.

5. Conclusion

The method of successive approximations has been used for the description of wave processes with weak nonlinearity. This method allows for simultaneous analyses of both the initial scattering field and the second

scattering field. The second field is considered as having only the difference frequency component. The diagrams are presented that illustrate the distribution of acoustic pressure of the scattered field. In view of the obtained theoretical results, the method of successive approximations is an adequate tool for solving the problem of the scattering of nonlinearly interacting waves by an elongated spheroid.

References

[1] R. Cpence, S. Ganger, The scattering of sound from a prolate spheroid, *Journal of the Acoustical Society of America* 23 (6) (1951) 701–706.
[2] A.A. Cleshev, L.S. Sheiba, The scattering of sound wave from an ideal elongated spheroids, *Acoustical Physics (Akusticheskii Zhurnal)* 16 (2) (1970) 264–268.
[3] M.V. Fedoryuk, The scattering of sound wave from thin acoustically rigid revolve body, *Akusticheskii Zhurnal* 27 (4) (1981) 605–609.
[4] A.I. Boiko, The scattering of plane sound wave from thin revolve body, *Akusticheskii Zhurnal* T29 (3) (1983) C321–C325.
[5] M.Yu. Tetyuchin, M.V. Fedoryuk, The diffraction of plane sound wave from a prolate rigid revolved body in the liquid, *Akusticheskii Zhurnal* 35 (1) (1989) 126–130.
[6] M.F. Werby, L.H. Green, Correspondence between acoustical scattering from spherical and end-on incidence spherical shells, *Journal of the Acoustical Society of America* 81 (2) (1987) 783–787.
[7] N.D. Weksler, B. Dubious, A. Lave, The scattering of acoustic wave from an ellipsoidal shell, *Akusticheskii Zhurnal* 45 (1) (1999) 53–58.
[8] A.V. Lebedev, B.M. Salin, An experimental method of definition of dispersion section of the prolate bodies, *Akusticheskii Zhurnal* 43 (3) (1997) 376–385.
[9] T.K. Stanton, Simple approximate formulas for backscattering of sound by spherical and elongated objects, *Journal of the Acoustical Society of America* 86 (4) (1989) 1499–1510.
[10] A.N. Tikhonov, A.A. Samarskyi, *The Equations of Mathematical Physics*, Nauka, Moscow, 1966 (724pp).
[11] E. Skudrzyk, *The Foundations of Acoustics*, Vol. 2, Springer, New York, 1971 (542pp).
[12] A.A. Cleshev, I.I. Clyukin, *The Foundation of Hydroacoustic*, Sudostroenie, Leningrad, 1987 (224pp).
[13] B.K. Novikov, O.V. Rudenko, V.I. Timoshenko, *Nonlinear Underwater Acoustic*, Acoustical Society of America, New York, 1987 (264pp).
[14] L.M. Lyamshev, P.V. Sakov, Nonlinear scattering of sound from an pulsted sphere, *Soviet Physics Acoustics* 38 (1) (1992) 51–57.
[15] H. Corn, T. Corn, *Handbook of the Mathematical*, Nauka, Moscow, 1968 (720pp).
[16] M. Abramovitz, I. Stegun, *Handbook of Special Functions with Formulas, Graphs, and Mathematical Tables*, Dover, New York, 1971 (830pp).
[17] A.P. Prudnikov, Yu.A. Brychkov, O.I. Marichhev, *Integrals and Rows*, Nauka, Moscow, 1983 (752pp).
[18] I.B. Abbasov, N.P. Zagrai, Scattering of interacting plane waves by a sphere, *Acoustical Physics* 40 (4) (1994) 473–479.
[19] I.B. Abbasov, N.P. Zagrai, The investigation of the second field of the summarized frequency originated from scattering of nonlinearly interacting sound waves at a rigid sphere, *Journal of Sound and Vibration* 216 (1) (1998) P194–P197.